

# Heterogeneous multicomponent nucleation theorems for the analysis of nanoclusters

Hanna Vehkamäki,<sup>a)</sup> Anni Määttänen,<sup>b)</sup> Antti Lauri, and Markku Kulmala  
*Department of Physical Sciences, P.O. Box 64, University of Helsinki, 00014 Helsinki, Finland*

Paul Winkler, Aron Vrtala, and Paul E. Wagner  
*Institut für Experimentalphysik, Universität Wien, Boltzmannngasse 5, A-1090 Vienna, Austria*

(Received 19 December 2006; accepted 15 March 2007; published online 7 May 2007)

In this paper we present a new form of the nucleation theorems applicable to heterogeneous nucleation. These heterogeneous nucleation theorems allow, for the first time, direct determination of properties of nanoclusters formed on pre-existing particles from measured heterogeneous nucleation probabilities. The theorems can be used to analyze the size (first theorem) and the energetics (second theorem) of heterogeneous clusters independent of any specific nucleation model. We apply the first theorem to the study of small water and *n*-propanol clusters formed at the surface of 8 nm silver particles. According to the experiments the size of the two-component critical clusters is found to be below 90 molecules, and only less than 20 molecules for pure water, less than 300 molecules for pure *n*-propanol. These values are drastically smaller than the ones predicted by the classical nucleation theory, which clearly indicates that the nucleating clusters are too small to be quantitatively described using a macroscopic theory. © 2007 American Institute of Physics. [DOI: 10.1063/1.2723073]

## I. INTRODUCTION

First-order phase transitions are crucial in many branches of physics and chemistry. The formation of a new phase can occur in a homogeneous parent phase or heterogeneously around some nucleation seeds such as impurities or particle surfaces.<sup>1</sup> In the case of gas-to-particle transition, condensation growth, evaporation, and heterogeneous chemistry are processes that define the fate of the newborn liquid or solid clusters after nucleation has occurred.<sup>2</sup> Nanoparticles have received intensive attention in many branches of technology, and heterogeneous nucleation is an important part of their formation processes. Atmospheric nanoparticles can affect human health, and when they grow to larger sizes they also reduce visibility and play a role in determining the Earth's radiation budget and thus climate change.<sup>3–6</sup> Recently, heterogeneous nucleation was suggested to be important in atmospheric nanoparticle formation.<sup>7</sup> We investigate the size of small clusters formed at the surface of a pre-existing aerosol particle. The number of molecules in a critical cluster—acting as a starting point of phase transition—can be obtained using the first nucleation theorem, which we derive here for heterogeneous nucleation. We also derive the second heterogeneous nucleation theorem, which gives the binding energy of the critical cluster, although experimental data for the application of this theorem does not yet exist. General forms for the nucleation theorems have been presented earlier,<sup>8</sup> but the lack of a specific form applicable to analysis of heterogeneous nucleation probability data has been hampering the use of these powerful analytical tools.

<sup>a)</sup>Electronic mail: hanna.vehkamaki@helsinki.fi

<sup>b)</sup>Also at: Finnish Meteorological Institute, P.O. Box 503, 00101 Helsinki, Finland

In Sec. II we review the general form for the first theorem, with temperature constant and varying gas-phase activities, in the case of heterogeneous nucleation, and in Sec. III we derive the general form for the second theorem studying a case where only temperature varies, but gas-phase activities are constant. In Secs. IV and V we show that the classical heterogeneous nucleation theory, and especially the geometric factors used in it, obey the form of the theorems. Section VI shows how the theorems are expressed in terms of the measurable nucleation probability, and Sec. VII discusses estimation of the role of the kinetic pre-factor. Section VIII describes the experimental results and how they are analyzed, and Sec. IX contains the results of the data analysis. In Sec. X we finally give conclusions.

## II. GENERAL FORMALISM: FIRST THEOREM

Kashchiev<sup>8</sup> has shown that for the isothermal case the nucleation theorem for heterogeneous gas-liquid multicomponent nucleation is

$$\left( \frac{\partial \Delta G_{\text{het}}^*}{\partial \mu^{g,i}} \right)_{T, \mu^{g,j \neq i}} = -\Delta N_{\text{het},i}^*, \quad (1)$$

where  $\Delta G_{\text{het}}^*$  is the formation free energy of the heterogeneous critical cluster,  $\mu^{g,i}$  is the gas-phase chemical potential of component *i*, *T* is the temperature, and

$$\Delta N_{\text{het},i}^* = N_{\text{het}}^{l,i} + N_{g,l,\text{het}}^{\text{surf},i} + N_{l,\text{sol}}^{\text{surf},i} - N_{g,\text{sol},A_{l,\text{sol}}}^{\text{surf},i} - V_{\text{het}}^l \rho_{g,i}, \quad (2)$$

is the excess number of molecules of component *i* in the critical cluster.  $N_{\text{het}}^{l,i}$  is the number of molecules in the bulk liquid phase of the cluster,  $N_{g,l,\text{het}}^{\text{surf},i}$  and  $N_{l,\text{sol}}^{\text{surf},i}$  are the numbers of molecules on the gas-liquid and liquid-solid surfaces of the cluster,  $N_{g,\text{sol},A_{l,\text{sol}}}^{\text{surf},i}$  is the number of molecules on a gas-

solid surface which has the same area  $A_{l,\text{sol}}$  as the liquid-solid interface of the cluster,  $V_{\text{het}}^l$  is the volume of the cluster, and  $\rho_{g,i}$  is the number density of component  $i$  in the gas phase. For gas-liquid surface and the liquid phase we have used the subscript  $\text{het}$  to explicitly indicate that we are dealing with the heterogeneous cluster, since also the homogeneous cluster has a gas-liquid interface and liquid phase core. In most cases we have omitted the superscript  $*$  referring to the critical cluster in the interest of simplifying the notations. All the quantities we deal with are those of the critical cluster unless otherwise stated.

In practice, experiments provide nucleation rate, or nucleation probability, as a function of gas-phase activities  $\mathcal{A}_{g,i}$ . The nucleation rate is proportional to  $\exp[-\Delta G_{\text{het}}^*/(kT)]$ , and the gas-phase activity is connected to the gas-phase chemical potential  $\mu^{g,i}$  by

$$\mu^{g,i} = \mu^{g,i,\text{pure}}(p_{\text{sat}}^{i,\text{pure}}) + kT \ln \mathcal{A}_{g,i}, \quad (3)$$

which is valid for an ideal mixture of ideal gases. The chemical potential of saturated pure vapor  $i$ ,  $\mu^{g,i,\text{pure}}(p_{\text{sat}}^{i,\text{pure}})$  depends only on temperature, and  $k$  is the Boltzmann constant. Using Eq. (3) the nucleation theorem (1) can be written as

$$\left( \frac{\partial \left( \frac{-\Delta G_{\text{het}}^*}{kT} \right)}{\partial \ln \mathcal{A}_{g,i}} \right)_{T, \mathcal{A}_{g,j \neq i}} = \Delta N_{\text{het},i}^* \quad (4)$$

For one-component systems  $\Delta N_{\text{het},i}^*$  given by (2) takes a simpler form  $\Delta N_{\text{het},i}^* = N_{\text{het}}^{l,i} - V_{\text{het}}^l \rho_{g,i}$  since the dividing surfaces between the phases can be chosen to be the equimolar surfaces,<sup>9</sup> and thus the numbers of surface molecules are zero. The homogeneous case is readily obtained as a special case of the heterogeneous theorem by setting the numbers of molecules on the gas-solid and liquid-solid interfaces as zero.

### III. GENERAL FORMALISM: SECOND THEOREM

The formation free energy of a heterogeneous critical cluster is

$$\Delta G_{\text{het}}^* = (P^g - P^l) V_{\text{het}}^l + \Phi, \quad (5)$$

where  $P^l$  and  $P^g$  are the pressure in the liquid cluster and the gas-phase pressure, respectively, and the effective surface energy<sup>8</sup> is

$$\Phi = \varphi_{l,\text{sol}} + \varphi_{g,l,\text{het}} - \varphi_{g,\text{sol},A_{l,\text{sol}}}, \quad (6)$$

where  $\varphi_{l,\text{sol}}$  is the contribution of the liquid-solid surface,  $\varphi_{g,l,\text{het}}$  is the contribution of the gas-liquid surface, and  $\varphi_{g,\text{sol},A_{l,\text{sol}}}$  is a contribution of a gas-solid surface which has the same area  $A_{l,\text{sol}}$  as the liquid-solid surface. The temperature derivative of the formation free energy is

$$\begin{aligned} \frac{\partial \Delta G_{\text{het}}^*}{\partial T} = & V_{\text{het}}^l \frac{\partial (P^g - P^l)}{\partial T} + (P^g - P^l) \frac{\partial V_{\text{het}}^l}{\partial T} + \frac{\partial \Phi}{\partial V_{\text{het}}^l} \frac{\partial V_{\text{het}}^l}{\partial T} \\ & + \left( \frac{\partial \Phi}{\partial T} \right)_{V_{\text{het}}^l}. \end{aligned} \quad (7)$$

The general expression for the formation free energy of a not necessarily critical cluster is<sup>9-11</sup>

$$\begin{aligned} \Delta G_{\text{het}} = & (P^g - P^l) V_{\text{het}}^l + \Phi + \sum_i (\mu^{l,i} - \mu^{g,i}) N_{\text{het}}^{l,i} \\ & + \sum_i (\mu_{l,\text{sol}}^{\text{surf},i} - \mu^{g,i}) N_{l,\text{sol}}^{\text{surf},i} + \sum_i (\mu_{g,\text{het}}^{\text{surf},i} \\ & - \mu^{g,i}) N_{g,l,\text{het}}^{\text{surf},i} - \sum_i (\mu_{g,\text{sol}}^{\text{surf},i} - \mu^{g,i}) N_{g,\text{sol},A_{l,\text{sol}}}^{\text{surf},i}. \end{aligned} \quad (8)$$

The critical cluster satisfies the condition  $(\partial \Delta G_{\text{het}}^* / \partial V_{\text{het}}^l)_{N_{\text{het}}^{l,i}, N_{l,\text{sol}}^{\text{surf},i}, N_{g,\text{sol}}^{\text{surf},i}, N_{g,l,\text{het}}^{\text{surf},i}} = 0$ , where the derivative is taken with respect to the location of the dividing surface, but keeping the actual physical cluster unchanged.<sup>12</sup> This leads to the generalized Laplace equation

$$(P^g - P^l) + \frac{\partial \Phi}{\partial V_{\text{het}}^l} = 0, \quad (9)$$

which is valid for the critical cluster, and any choice of the dividing surface,<sup>10</sup> and thus Eq. (7) reduces to

$$\frac{\partial \Delta G_{\text{het}}^*}{\partial T} = V_{\text{het}}^l \frac{\partial (P^g - P^l)}{\partial T} + \left( \frac{\partial \Phi}{\partial T} \right)_{V_{\text{het}}^l}. \quad (10)$$

For each surface phase we use the Gibbs' adsorption equation, which in a nonisothermal case reads

$$d\Phi|_A = -S^{\text{surf}} dT - \sum_i d\mu^{\text{surf},i} N^{\text{surf},i}, \quad (11)$$

where  $S$  stands for entropy, and for the bulk liquid and gas we have the Gibbs-Duhem equations

$$V_{\text{het}}^l dP^l = S_{\text{het}}^l dT + \sum_i d\mu^{l,i} N_{\text{het}}^{l,i} \quad (12)$$

and

$$V_{\text{het}}^g dP^g = S_{\text{het}}^g dT + \sum_i d\mu^{g,i} N_{\text{het}}^{g,i}, \quad (13)$$

where  $V_{\text{het}}^g$  is the gas-phase volume and  $N_{\text{het}}^{g,i} = V_{\text{het}}^g \rho_{g,i}$  is the number of gas molecules. Assuming that keeping the volume constant also keeps the surface area constant (in other words the shape of the cluster is unchanged) Eq. (10) can then be written as

$$\begin{aligned} \frac{\partial \Delta G_{\text{het}}^*}{\partial T} = & \frac{V_{\text{het}}^l}{V_{\text{het}}^g} \left( S_{\text{het}}^g + \sum_i N_{\text{het}}^{g,i} \frac{\partial \mu^{g,i}}{\partial T} \right) \\ & - \left( S_{\text{het}}^l + \sum_i N_{\text{het}}^{l,i} \frac{\partial \mu^{l,i}}{\partial T} \right) \\ & - \left( S_{l,\text{sol}}^{\text{surf}} + \sum_i N_{l,\text{sol}}^{\text{surf},i} \frac{\partial \mu_{l,\text{sol}}^{\text{surf},i}}{\partial T} \right) \\ & - \left( S_{g,l,\text{het}}^{\text{surf}} + \sum_i N_{g,l,\text{het}}^{\text{surf},i} \frac{\partial \mu_{g,l,\text{het}}^{\text{surf},i}}{\partial T} \right) \\ & + \left( S_{g,\text{sol},A_{l,\text{sol}}}^{\text{surf}} + \sum_i N_{g,\text{sol},A_{l,\text{sol}}}^{\text{surf},i} \frac{\partial \mu_{g,\text{sol}}^{\text{surf},i}}{\partial T} \right), \end{aligned} \quad (14)$$

where  $S_{g,\text{sol},A_{l,\text{sol}}}^{\text{surf}}$  is the entropy of a gas-solid surface which has area  $A_{l,\text{sol}}$ .

The critical cluster is in a metastable equilibrium with the vapor, and thus the chemical potentials are equal throughout the system

$$\mu_{l,\text{sol}}^{\text{surf},i} = \mu_{g,l,\text{het}}^{\text{surf},i} = \mu_{g,\text{sol}}^{\text{surf},i} = \mu^{l,i} = \mu^{g,i}. \quad (15)$$

If the gas-phase chemical potentials are kept constant while taking the derivative with respect to temperature, the second nucleation theorem is simply

$$\left(\frac{\partial \Delta G_{\text{het}}^*}{\partial T}\right)_{\mu^{g,i}} = -S_{\text{het}}^l - S_{l,\text{sol}}^{\text{surf}} - S_{g,l,\text{het}}^{\text{surf}} + \frac{V_{\text{het}}^l}{V_{\text{het}}^g} S^g + S_{g,\text{sol},A_{l,\text{sol}}}^{\text{surf}}. \quad (16)$$

In Eq. (16), the combination of the negative terms give the total entropy of the heterogeneous critical cluster, and the positive terms the entropy that the space which the cluster occupies (volume  $V_{\text{het}}^l$  and the surface area  $A_{l,\text{sol}}$ ) when filled with the gas phase, and thus the equation can be written

$$\left(\frac{\partial \Delta G_{\text{het}}^*}{\partial T}\right)_{\mu^{g,i}} = -\Delta S^*. \quad (17)$$

In practical applications it is however more convenient to keep the gas-phase activities, rather than the chemical potentials, constant and Eq. (3) together with the Gibbs-Duhem equation and Clausius-Clapeyron equation allow then the temperature derivative of the gas-phase chemical potential to be expressed as<sup>13</sup>

$$\left(\frac{d\mu^{g,i}}{dT}\right)_{A_{g,i}} \approx \frac{\mu^{g,i}}{T} - \frac{h_{\text{pure}}^{l,i}}{T} \approx \frac{\mu^{g,i}}{T} - \frac{e_{\text{pure}}^{l,i}}{T}, \quad (18)$$

where  $h_{\text{pure}}^{l,i}$  and  $e_{\text{pure}}^{l,i}$  are the enthalpy and energy, respectively, per molecule in a pure bulk liquid  $i$ . In deriving the first equality of result (18), the partial molecular volume in the liquid has been assumed negligible compared to the partial molecular volume in the gas. Using (15) and (18) in Eq. (14) results in

$$\begin{aligned} \left(\frac{\partial \Delta G_{\text{het}}^*}{\partial T}\right)_{A_{g,i}} &= \frac{1}{T} \left[ \frac{V_{\text{het}}^l}{V_{\text{het}}^g} \left( TS^g + \sum_i N_{\text{het}}^{g,i} (\mu^{g,i} - e_{\text{pure}}^{l,i}) \right) - \left( TS_{\text{het}}^l + \sum_i N_{\text{het}}^{l,i} (\mu^{l,i} - e_{\text{pure}}^{l,i}) \right) - \left( TS_{l,\text{sol}}^{\text{surf}} + \sum_i N_{l,\text{sol}}^{\text{surf},i} (\mu_{l,\text{sol}}^{\text{surf},i} - e_{\text{pure}}^{l,i}) \right) \right. \\ &\quad \left. - \left( TS_{g,l,\text{het}}^{\text{surf}} + \sum_i N_{g,l,\text{het}}^{\text{surf},i} (\mu_{g,l,\text{het}}^{\text{surf},i} - e_{\text{pure}}^{l,i}) \right) + \left( TS_{g,\text{sol},A_{l,\text{sol}}}^{\text{surf}} + \sum_i N_{g,\text{sol},A_{l,\text{sol}}}^{\text{surf},i} (\mu_{g,\text{sol}}^{\text{surf},i} - e_{\text{pure}}^{l,i}) \right) \right]. \quad (19) \end{aligned}$$

For the derivative of the nucleation rate (or the nucleation probability) we need again the derivative of  $-\Delta G_{\text{het}}^*/(kT)$  which, using the critical cluster formation energy given by Eq. (5), can be written as

$$\begin{aligned} \left(\frac{\partial \frac{-\Delta G_{\text{het}}^*}{kT}}{\partial T}\right)_{A_{g,i}} &= \frac{-1}{kT} \left(\frac{\partial \Delta G_{\text{het}}^*}{\partial T}\right)_{A_{g,i}} + \frac{\Delta G_{\text{het}}^*}{kT^2} = \frac{1}{kT^2} \left[ \Delta G_{\text{het}}^* - T \left(\frac{\partial \Delta G_{\text{het}}^*}{\partial T}\right)_{A_{g,i}} \right] \\ &= \left[ \frac{-V_{\text{het}}^l}{V_{\text{het}}^g} \left( -P^g V_{\text{het}}^g + TS^g + \sum_i N_{\text{het}}^{g,i} (\mu^{g,i} - e_{\text{pure}}^{l,i}) \right) + \left( -P^l V_{\text{het}}^l + TS_{\text{het}}^l + \sum_i N_{\text{het}}^{l,i} (\mu^{l,i} - e_{\text{pure}}^{l,i}) \right) \right. \\ &\quad \left. + \left( \varphi_{l,\text{sol}} + TS_{l,\text{sol}}^{\text{surf}} + \sum_i N_{l,\text{sol}}^{\text{surf},i} (\mu_{l,\text{sol}}^{\text{surf},i} - e_{\text{pure}}^{l,i}) \right) + \left( \varphi_{g,l,\text{het}} + TS_{g,l,\text{het}}^{\text{surf}} + \sum_i N_{g,l,\text{het}}^{\text{surf},i} (\mu_{g,l,\text{het}}^{\text{surf},i} - e_{\text{pure}}^{l,i}) \right) \right. \\ &\quad \left. - \left( \varphi_{g,\text{sol},A_{l,\text{sol}}} + TS_{g,\text{sol},A_{l,\text{sol}}}^{\text{surf}} + \sum_i N_{g,\text{sol},A_{l,\text{sol}}}^{\text{surf},i} (\mu_{g,\text{sol}}^{\text{surf},i} - e_{\text{pure}}^{l,i}) \right) \right] \frac{1}{kT^2}. \quad (20) \end{aligned}$$

With the help of the total energy of a surface phase

$$U^{\text{surf}} = \varphi + TS^{\text{surf}} + \sum_i \mu^{\text{surf},i} N^{\text{surf},i}, \quad (21)$$

and the energies of liquid and gas phases

$$\begin{aligned} U^l &= -P^l V_{\text{het}}^l + TS^l + \sum_i \mu^{l,i} N^{l,i}, \\ U^g &= -P^g V_{\text{het}}^g + TS^g + \sum_i \mu^{g,i} N_{\text{het}}^{g,i}, \quad (22) \end{aligned}$$

Equation (20) can be written as

$$\begin{aligned} \left(\frac{\partial \frac{-\Delta G_{\text{het}}^*}{kT}}{\partial T}\right)_{A_{g,i}} &= \frac{1}{kT^2} \left( U_{\text{het}}^l + U_{g,l,\text{het}}^{\text{surf}} + U_{l,\text{sol}}^{\text{surf}} - \frac{V_{\text{het}}^l}{V_{\text{het}}^g} U^g \right. \\ &\quad \left. - U_{g,\text{sol},A_{l,\text{sol}}}^{\text{surf}} - \sum_i e_{\text{pure}}^{l,i} N_{\text{het}}^{l,i} \right. \\ &\quad \left. - \sum_i e_{\text{pure}}^{l,i} N_{g,l,\text{het}}^{\text{surf},i} - \sum_i e_{\text{pure}}^{l,i} N_{l,\text{sol}}^{\text{surf},i} \right. \\ &\quad \left. + \frac{V_{\text{het}}^l}{V_{\text{het}}^g} \sum_i e_{\text{pure}}^{l,i} N_{\text{het}}^{g,i} + \sum_i e_{\text{pure}}^{l,i} N_{g,\text{sol},A_{l,\text{sol}}}^{\text{surf},i} \right). \quad (23) \end{aligned}$$

In Eq. (23) the first three terms give the total energy of the

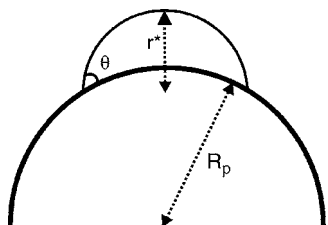


FIG. 1. Geometry of a cluster (cap-shaped part of a sphere with radius  $r^*$ ) forming on a spherical seed particle with radius  $R_p$ .  $\theta$  is the contact angle.

heterogeneous cluster; the next two terms represent the energy that the space occupied by the cluster would have if filled with gas; the last five terms give the energy the cluster molecules would have in pure bulk liquids, and the energy the molecules in the gas-filled cluster volume and on the gas-solid surface would have in pure bulk liquids. Thus a simple form for the second nucleation theorem reads

$$\left(\frac{\partial\left(\frac{-\Delta G_{\text{het}}^*}{kT}\right)}{\partial T}\right)_{\mathcal{A}_{g,i}} = \frac{\Delta(\Delta_{\text{pure},l}U^*)}{kT^2}, \quad (24)$$

where  $\Delta_{\text{pure},l}$  refers to the difference compared to pure liquids, and the first  $\Delta$  refers to the difference between the cluster and the same space occupied by gas phase. For one-component system the theorem (23) can be simplified, since by using equimolar surfaces as the dividing surfaces the numbers of molecules on the surfaces can be set to zero. The homogeneous case is again obtained as a special case of the heterogeneous theorem by setting the energies and numbers of molecules related to the gas-solid and liquid-solid interfaces as zero. For comparison with earlier forms of second homogeneous nucleation theorem, see remarks after Eq. (55).

#### IV. CLASSICAL FORMALISM: FIRST THEOREM

In the classical heterogeneous nucleation theory the nucleating cluster is treated as a cap-shaped embryo with radius  $r^*$  forming on a spherical seed particle with radius  $R_p$ , and the contact angle between the cluster and the underlying surface is denoted by  $\theta$ . Figure 1 shows the geometry of the situation. This geometry is a special case of a more general situation governed by the results in the preceding sections. We also want to show that the well-known geometric factors<sup>14</sup> arising in this special case can explicitly be manipulated so that we arrive in the heterogeneous nucleation theorems.

In the same gas-phase activities and temperature, the radius of the heterogeneous cluster is the same as that of the homogeneous one, and it is given by the Kelvin equation

$$r^* = \frac{2v_{l,i}\sigma_{g,l}}{kT \ln \mathcal{A}_{g,i}/\mathcal{A}_{l,i}}, \quad (25)$$

where  $v_{l,i}$  and  $\mathcal{A}_{l,i}$  are, respectively, the liquid phase partial molecular volume activity of component  $i$ ,  $\sigma_{g,l}$  is the gas-liquid surface tension,  $k$  is the Boltzmann constant and  $T$  is the temperature. The critical cluster composition can be solved from equation

$$\frac{v_{l,i}}{kT \ln \mathcal{A}_{g,i}/\mathcal{A}_{l,i}} = \frac{v_{l,j}}{kT \ln \mathcal{A}_{g,j}/\mathcal{A}_{l,j}}. \quad (26)$$

For the homogeneous critical cluster the formation energy can be written as

$$\frac{\Delta G_{\text{hom}}^*}{kT} = \frac{4\pi r^{*2}\sigma_{g,l}}{3kT}. \quad (27)$$

The first homogeneous nucleation theorem<sup>10</sup> gives the excess (compared to the cluster volume filled with vapor) number of component  $i$  molecules in the critical cluster as

$$\begin{aligned} -\Delta N_{\text{hom},i}^* &= \left(\frac{\partial\left(\frac{\Delta G_{\text{hom}}^*}{kT}\right)}{\partial \ln \mathcal{A}_{g,i}}\right)_{T,\mathcal{A}_{g,j\neq i}} \\ &= \frac{4\pi r^{*2}\sigma_{g,l}}{3kT} \left(\frac{2}{r^*} \frac{\partial r^*}{\partial \ln \mathcal{A}_{g,i}} + \frac{1}{\sigma_{g,l}} \frac{\partial \sigma_{g,l}}{\partial \ln \mathcal{A}_{g,i}}\right). \end{aligned} \quad (28)$$

The formation energy for a heterogeneous critical cluster can be expressed with the help of the homogeneous formation energy as<sup>14</sup>

$$\Delta G_{\text{het}}^* = f_G \Delta G_{\text{hom}}^*. \quad (29)$$

The geometric factor  $f_G$  can be expressed as<sup>14</sup>

$$\begin{aligned} f_G &= \frac{1}{2} \left\{ 1 + \left(\frac{1-Xm}{g}\right)^3 + X^3 \left[ 2 - 3\left(\frac{X-m}{g}\right) \right. \right. \\ &\quad \left. \left. + \left(\frac{X-m}{g}\right)^3 \right] + 3X^2m \left(\frac{X-m}{g} - 1\right) \right\}, \end{aligned} \quad (30)$$

where  $g = \sqrt{1+X^2-2Xm}$ ,

$$X = \frac{R_p}{r^*}, \quad (31)$$

and the contact parameter is  $m = \cos \theta$ . Young's equation<sup>15</sup> relates the contact parameter to the surface tensions between gas and solid ( $\sigma_{g,\text{sol}}$ ), liquid and solid ( $\sigma_{l,\text{sol}}$ ), and gas and liquid ( $\sigma_{g,l}$ ) as

$$m = \cos \theta = \frac{\sigma_{g,\text{sol}} - \sigma_{l,\text{sol}}}{\sigma_{g,l}}. \quad (32)$$

The number of molecules in the liquid phase of the heterogeneous critical cluster is connected to the homogeneous case by  $N_{\text{het}}^{l,i} = f_N N_{\text{hom}}^{l,i}$ , where  $f_N$  is the ratio of heterogeneous and homogeneous cluster volumes,  $V_{\text{het}}^l$  and  $V_{\text{hom}}^l$ , assuming the same liquid density in both cases<sup>14,16</sup>

$$\begin{aligned} f_N &= \frac{V_{\text{het}}^l}{V_{\text{hom}}^l} = \frac{1}{4} \left\{ 2 + 3\left(\frac{1-Xm}{g}\right) - \left(\frac{1-Xm}{g}\right)^3 \right. \\ &\quad \left. - X^3 \left[ 2 - 3\left(\frac{X-m}{g}\right) + \left(\frac{X-m}{g}\right)^3 \right] \right\}. \end{aligned} \quad (33)$$

For a planar pre-existing surface  $X \rightarrow \infty$  and  $f_G = f_N$ , but for a spherical condensation nucleus  $f_G \neq f_N$ .

Using the equality of chemical potentials (15), gas-phase chemical potential (3) and  $\Phi = A\sigma$ , Gibbs adsorption Eq. (11) at constant temperature leads to equations

$$A_{l,\text{sol}} \frac{\partial \sigma_{l,\text{sol}}}{\partial \ln \mathcal{A}_{g,i}} = -kTN_{l,\text{sol}}^{\text{surf},i}, \quad (34)$$

$$A_{l,\text{sol}} \frac{\partial \sigma_{g,\text{sol}}}{\partial \ln \mathcal{A}_{g,i}} = -kTN_{g,\text{sol},A_{l,\text{sol}}}^{\text{surf},i}, \quad (35)$$

$$A_{g,l}^{\text{hom}} \frac{\partial \sigma_{g,\text{sol}}}{\partial \ln \mathcal{A}_{g,i}} = 4\pi r^{*2} \frac{\partial \sigma_{g,\text{sol}}}{\partial \ln \mathcal{A}_{g,i}} = -kTN_{g,l,\text{hom}}^{\text{surf},i}, \quad (36)$$

where the surface area of the homogeneous cluster is

$$A_{g,l}^{\text{hom}} = 4\pi r^{*2}. \quad (37)$$

The gas-liquid surface area in the heterogeneous case is

$$A_{g,l}^{\text{het}} = 2\pi r^{*2} \left( 1 - \frac{mX-1}{g} \right). \quad (38)$$

The liquid-solid interface area is

$$A_{l,\text{sol}} = 2\pi R_p^2 \left( 1 - \frac{X-m}{g} \right), \quad (39)$$

and thus the derivative of the factor  $f_G$  with respect to contact parameter  $m$  can be expressed as

$$\frac{4\pi r^{*2}}{3} \frac{\partial f_G}{\partial m} = 2\pi R_p^2 \left( \frac{X-m}{g} - 1 \right) = -A_{l,\text{sol}}. \quad (40)$$

Young's Eq. (32) gives

$$\frac{\partial m}{\partial \ln \mathcal{A}_{g,i}} = \frac{1}{\sigma_{g,l}} \left( \frac{\partial(\sigma_{g,\text{sol}} - \sigma_{l,\text{sol}})}{\partial \ln \mathcal{A}_{g,i}} - m \frac{\partial \sigma_{g,l}}{\partial \ln \mathcal{A}_{g,i}} \right), \quad (41)$$

and Eq. (31)

$$\frac{\partial X}{\partial r^*} = -\frac{R_p}{r^{*2}} = -\frac{X}{r^*}. \quad (42)$$

The dependence of the heterogeneous cluster formation free energy on the gas-phase activity  $\mathcal{A}_{g,i}$  is given by

$$\begin{aligned} \left( \frac{\partial \left( \frac{-\Delta G_{\text{het}}^*}{kT} \right)}{\partial \ln \mathcal{A}_{g,i}} \right)_{T, \mathcal{A}_{g,j \neq i}} &= -f_G \frac{\partial \left( \frac{\Delta G_{\text{hom}}^*}{kT} \right)}{\partial \ln \mathcal{A}_{g,i}} - \frac{\Delta G_{\text{hom}}^*}{kT} \left( \frac{\partial f_G}{\partial X} \frac{\partial X}{\partial r^*} \frac{\partial r^*}{\partial \ln \mathcal{A}_{g,i}} + \frac{\partial f_G}{\partial m} \frac{\partial m}{\partial \ln \mathcal{A}_{g,i}} \right) \\ &= f_G \Delta N_{\text{hom}}^* + \frac{\Delta G_{\text{hom}}^*}{kT} \left( \frac{X}{r^*} \frac{\partial f_G}{\partial X} \frac{\partial r^*}{\partial \ln \mathcal{A}_{g,i}} + \frac{m}{\sigma_{g,l}} \frac{\partial f_G}{\partial m} \frac{\partial \sigma_{g,l}}{\partial \ln \mathcal{A}_{g,i}} - \frac{1}{\sigma_{g,l}} \frac{\partial f_G}{\partial m} \frac{\partial(\sigma_{g,\text{sol}} - \sigma_{l,\text{sol}})}{\partial \ln \mathcal{A}_{g,i}} \right) \\ &= f_G \Delta N_{\text{hom}}^* + \frac{X}{2} \frac{\partial f_G}{\partial X} \frac{4\pi r^{*2} \sigma_{g,l}}{3kT} \left( \frac{2}{r^*} \frac{\partial r^*}{\partial \ln \mathcal{A}_{g,i}} + \frac{1}{\sigma_{g,l}} \frac{\partial \sigma_{g,l}}{\partial \ln \mathcal{A}_{g,i}} \right) + \frac{4\pi r^{*2}}{3kT} \left[ \left( m \frac{\partial f_G}{\partial m} - \frac{X}{2} \frac{\partial f_G}{\partial X} \right) \frac{\partial \sigma_{g,l}}{\partial \ln \mathcal{A}_{g,i}} \right. \\ &\quad \left. - \frac{\partial f_G}{\partial m} \frac{\partial(\sigma_{g,\text{sol}} - \sigma_{l,\text{sol}})}{\partial \ln \mathcal{A}_{g,i}} \right], \end{aligned} \quad (43)$$

where in the last stage we have added and subtracted term  $4\pi r^{*2}/(3kT)(X/2)(\partial f_G/\partial X)(\partial \sigma_{g,l}/\partial \ln \mathcal{A}_{g,i})$  to be able to identify the last form of Eq. (28). Using Eqs. (28), (34)–(36), and (40), Eq. (43) can be transformed to read

$$\begin{aligned} \left( \frac{\partial \left( \frac{-\Delta G_{\text{het}}^*}{kT} \right)}{\partial \ln \mathcal{A}_{g,i}} \right)_{T, \mathcal{A}_{g,j \neq i}} &= \left( f_G - \frac{X}{2} \frac{\partial f_G}{\partial X} \right) \Delta N_{\text{hom}}^* \\ &\quad - \frac{1}{3} \left( m \frac{\partial f_G}{\partial m} - \frac{X}{2} \frac{\partial f_G}{\partial X} \right) N_{g,l,\text{hom}}^{\text{surf},i} \\ &\quad + N_{l,\text{sol}}^{\text{surf},i} - N_{g,\text{sol},A_{l,\text{sol}}}^{\text{surf},i} \\ &= f_N \Delta N_{\text{hom}}^* - \frac{1}{3} \left( m \frac{\partial f_G}{\partial m} - \frac{X}{2} \frac{\partial f_G}{\partial X} \right) N_{g,l,\text{hom}}^{\text{surf},i} \\ &\quad + N_{l,\text{sol}}^{\text{surf},i} - N_{g,\text{sol},A_{l,\text{sol}}}^{\text{surf},i}, \end{aligned} \quad (44)$$

where we have used the following relation between the geometrical factors:

$$\left( f_G - \frac{X}{2} \frac{\partial f_G}{\partial X} \right) = f_N. \quad (45)$$

The excess number of molecules in the homogeneous cluster consists of bulk liquid ( $N_{\text{hom}}^{l,i}$ ) and surface phase ( $N_{g,l,\text{hom}}^{\text{surf},i}$ ) contributions

$$\Delta N_{\text{hom}}^* = N_{\text{hom}}^{l,i} + N_{g,l,\text{hom}}^{\text{surf},i} - V_{\text{hom}}^l \rho_{g,i}. \quad (46)$$

Equation (44) can then be written as

$$\begin{aligned} \left( \frac{\partial \left( \frac{-\Delta G_{\text{het}}^*}{kT} \right)}{\partial \ln \mathcal{A}_{g,i}} \right)_{T, \mathcal{A}_{g,j \neq i}} &= f_N N_{\text{hom}}^{l,i} + \left[ f_N - \frac{1}{3} \left( m \frac{\partial f_G}{\partial m} - \frac{X}{2} \frac{\partial f_G}{\partial X} \right) \right] \\ &\quad \times N_{g,l,\text{hom}}^{\text{surf},i} + N_{l,\text{sol}}^{\text{surf},i} - N_{g,\text{sol},A_{l,\text{sol}}}^{\text{surf},i} \\ &\quad - f_N V_{\text{hom}}^l \rho_{g,i}. \end{aligned} \quad (47)$$

Using surface areas (37) and (38) we get

$$f_N - \frac{1}{3} \left( m \frac{\partial f_G}{\partial m} - \frac{X}{2} \frac{\partial f_G}{\partial X} \right) = \frac{1}{2} \left( \frac{1-mX+g}{g} \right) = \frac{A_{g,l}^{\text{het}}}{A_{g,l}^{\text{hom}}}, \quad (48)$$

and the first heterogeneous nucleation theorem takes the general form (4)



$$\begin{aligned} \left( \frac{\partial \left( \frac{-\Delta G_{\text{het}}^*}{kT} \right)}{\partial \ln \mathcal{A}_{g,i}} \right)_{T, \mathcal{A}_{g,j \neq i}} &= f_N N_{\text{hom}}^{l,i} + \frac{A_{g,l}^{\text{het}}}{A_{g,l}^{\text{hom}}} N_{g,l,\text{hom}}^{\text{surf},i} + N_{l,\text{sol}}^{\text{surf},i} \\ &\quad - N_{g,\text{sol},A_{l,\text{sol}}}^{\text{surf},i} - f_N V_{\text{hom}}^l \rho_{g,i} \\ &= N_{\text{het}}^{l,i} + N_{g,l,\text{het}}^{\text{surf},i} + N_{l,\text{sol}}^{\text{surf},i} - N_{g,\text{sol},A_{l,\text{sol}}}^{\text{surf},i} \\ &\quad - V_{\text{het}}^l \rho_{g,i} = \Delta N_{\text{het}}^*, \end{aligned} \quad (49)$$

where we have used relations  $A_{g,l}^{\text{het}}/A_{g,l}^{\text{hom}} N_{g,l,\text{hom}}^{\text{surf},i} = N_{g,l,\text{het}}^{\text{surf},i}$ ,  $f_N N_{\text{hom}}^{l,i} = N_{\text{het}}^{l,i}$ , and  $f_N V_{\text{hom}}^l = V_{\text{het}}^l$ . This result concludes that the classical Fletcher<sup>14</sup> theory for heterogeneous nucleation, and the frequently used geometrical factors involved, are consistent with the first nucleation theorem.

## V. CLASSICAL FORMALISM: SECOND THEOREM

The second homogeneous nucleation theorem<sup>13</sup> relates the temperature derivative of the formation free energy to the excess energy of the critical cluster compared to the same molecules in pure bulk liquids

$$\begin{aligned} -\frac{\Delta U_{\text{hom}}^*}{kT^2} &= \left( \frac{\partial \left( \frac{\Delta G_{\text{hom}}^*}{kT} \right)}{\partial T} \right)_{\mathcal{A}_{g,i}} \\ &= \frac{4\pi r^{*2} \sigma_{g,l}}{3kT} \left( \frac{2}{r^*} \frac{\partial r^*}{\partial T} + \frac{1}{\sigma_{g,l}} \frac{\partial \sigma_{g,l}}{\partial T} - \frac{1}{T} \right). \end{aligned} \quad (50)$$

Using equality of chemical potentials (15) and formula (18) for the temperature derivative of the chemical potential in the Gibbs adsorption Eq. (11) in a nonisothermal case with  $\Phi = A\sigma$  thus leads to equation

$$\begin{aligned} A \left( \frac{\partial \sigma}{\partial T} \right)_{\mathcal{A}_{g,i}} &= -S^{\text{surf}} - \sum_i N^{\text{surf},i} \left( \frac{\partial \mu^{\text{surf},i}}{\partial T} \right)_{\mathcal{A}_{g,i}} \\ &= -\frac{1}{T} \left( TS^{\text{surf}} + \sum_i \mu^{\text{surf},i} N^{\text{surf},i} - \sum_i e_{\text{pure}}^{l,i} N^{\text{surf},i} \right) \\ &= -\frac{1}{T} \left( U^{\text{surf}} - A\sigma - \sum_i e_{\text{pure}}^{l,i} N^{\text{surf},i} \right), \end{aligned} \quad (51)$$

where we have used Eq. (21) for the surface phase energy. Young's Eq. (32) gives

$$\frac{\partial m}{\partial T} = \frac{1}{\sigma_{g,l}} \left( \frac{\partial (\sigma_{g,\text{sol}} - \sigma_{l,\text{sol}})}{\partial T} - m \frac{\partial \sigma_{g,l}}{\partial T} \right). \quad (52)$$

The temperature derivative of the formation free energy is

$$\begin{aligned} \left( \frac{\partial \left( \frac{-\Delta G_{\text{het}}^*}{kT} \right)}{\partial T} \right)_{\mathcal{A}_{g,i}} &= -f_G \frac{\partial \left( \frac{\Delta G_{\text{hom}}^*}{kT} \right)}{\partial T} - \frac{\Delta G_{\text{hom}}^*}{kT} \left( \frac{\partial f_G}{\partial X} \frac{\partial X}{\partial r^*} \frac{\partial r^*}{\partial T} + \frac{\partial f_G}{\partial m} \frac{\partial m}{\partial T} \right) \\ &= f_G \frac{\Delta U_{\text{hom}}^*}{kT^2} + \frac{\Delta G_{\text{hom}}^*}{kT} \left( \frac{X}{r^*} \frac{\partial f_G}{\partial X} \frac{\partial r^*}{\partial T} + \frac{m}{\sigma_{g,l}} \frac{\partial f_G}{\partial m} \frac{\partial \sigma_{g,l}}{\partial T} - \frac{1}{\sigma_{g,l}} \frac{\partial f_G}{\partial m} \frac{\partial (\sigma_{g,\text{sol}} - \sigma_{l,\text{sol}})}{\partial T} \right) \\ &= f_G \frac{\Delta U_{\text{hom}}^*}{kT^2} + \frac{X}{2} \frac{\partial f_G}{\partial X} \frac{4\pi r^{*2} \sigma_{g,l}}{3kT} \left( \frac{2}{r^*} \frac{\partial r^*}{\partial T} + \frac{1}{\sigma_{g,l}} \frac{\partial \sigma_{g,l}}{\partial T} - \frac{1}{T} \right) + \frac{4\pi r^{*2} \sigma_{g,l}}{3kT^2} \frac{X}{2} \frac{\partial f_G}{\partial X} + \frac{4\pi r^{*2}}{3kT} \\ &\quad \times \left[ \left( m \frac{\partial f_G}{\partial m} - \frac{X}{2} \frac{\partial f_G}{\partial X} \right) \frac{\partial \sigma_{g,l}}{\partial T} - \frac{\partial f_G}{\partial m} \frac{\partial (\sigma_{g,\text{sol}} - \sigma_{l,\text{sol}})}{\partial T} \right], \end{aligned} \quad (53)$$

where we have added and subtracted terms  $4\pi r^{*2}/(3kT)(X/2)(\partial f_G/\partial X)[(1/\sigma_{g,l})(\partial \sigma_{g,l}/\partial T) - 1/T]$  to be able to identify the last form of Eq. (50). Using Eqs. (50), (45), (40), (37), and (51) for homogeneous gas-liquid and heterogeneous gas-solid and liquid-solid surfaces, Eq. (53) can be written as

$$\begin{aligned} \left( \frac{\partial \left( \frac{-\Delta G_{\text{het}}^*}{kT} \right)}{\partial T} \right)_{\mathcal{A}_{g,i}} &= \left( f_G - \frac{X}{2} \frac{\partial f_G}{\partial X} \right) \frac{\Delta U_{\text{hom}}^*}{kT^2} + \frac{1}{3kT} \left( m \frac{\partial f_G}{\partial m} - \frac{X}{2} \frac{\partial f_G}{\partial X} \right) A_{g,l}^{\text{hom}} \frac{\partial \sigma_{g,l}}{\partial T} + \frac{A_{g,l}^{\text{hom}} \sigma_{g,l} X}{3kT^2} \frac{\partial f_G}{\partial X} + \frac{A_{l,\text{sol}}}{kT} \frac{\partial (\sigma_{g,\text{sol}} - \sigma_{l,\text{sol}})}{\partial T} \\ &= f_N \frac{\Delta U_{\text{hom}}^*}{kT^2} - \frac{1}{3kT^2} \left( m \frac{\partial f_G}{\partial m} - \frac{X}{2} \frac{\partial f_G}{\partial X} \right) \times \left( U_{g,l,\text{hom}}^{\text{surf}} - A_{g,l}^{\text{hom}} \sigma_{g,l} - \sum_i e_{\text{pure}}^{l,i} N_{g,l,\text{hom}}^{\text{surf},i} \right) + \frac{A_{g,l}^{\text{hom}} \sigma_{g,l} X}{3kT^2} \frac{\partial f_G}{\partial X} \\ &\quad - \frac{1}{kT^2} \left( U_{g,\text{sol},A_{l,\text{sol}}}^{\text{surf}} - A_{l,\text{sol}} \sigma_{g,\text{sol}} - \sum_i e_{\text{pure}}^{l,i} N_{g,\text{sol},A_{l,\text{sol}}}^{\text{surf},i} - U_{l,\text{sol}}^{\text{surf}} + A_{l,\text{sol}} \sigma_{l,\text{sol}} + \sum_i e_{\text{pure}}^{l,i} N_{l,\text{sol}}^{\text{surf},i} \right) \\ &= f_N \frac{\Delta U_{\text{hom}}^*}{kT^2} - \frac{U_{g,l,\text{hom}}^{\text{surf}} - \sum_i e_{\text{pure}}^{l,i} N_{g,l,\text{hom}}^{\text{surf},i}}{3kT^2} \left( m \frac{\partial f_G}{\partial m} - \frac{X}{2} \frac{\partial f_G}{\partial X} \right) - \frac{1}{kT^2} m \sigma_{g,l} A_{l,\text{sol}} - \frac{1}{kT^2} A_{l,\text{sol}} (-\sigma_{g,\text{sol}} + \sigma_{l,\text{sol}}) \\ &\quad - \left( \frac{U_{g,\text{sol},A_{l,\text{sol}}}^{\text{surf}} - \sum_i e_{\text{pure}}^{l,i} N_{g,\text{sol},A_{l,\text{sol}}}^{\text{surf},i}}{kT^2} \right) + \frac{U_{l,\text{sol}}^{\text{surf}} - \sum_i e_{\text{pure}}^{l,i} N_{l,\text{sol}}^{\text{surf},i}}{kT^2}. \end{aligned} \quad (54)$$

The combination of terms proportional to  $A_{l,\text{sol}}$  equals zero according to Young's Eq. (32). The excess energy of the homogeneous cluster consists of bulk liquid ( $U_{\text{hom}}^l$ ) and surface phase ( $U_{g,l,\text{hom}}^{\text{surf},i}$ ) contributions

$$\begin{aligned} \Delta U_{\text{hom}}^* &= U_{\text{hom}}^l + U_{g,l,\text{hom}}^{\text{surf}} - \frac{V_{\text{hom}}^l}{V_{\text{hom}}^g} U^g - \sum_i e_{\text{pure}}^{l,i} N_{\text{hom}}^{l,i} \\ &\quad - \sum_i e_{\text{pure}}^{l,i} N_{g,l,\text{hom}}^{\text{surf},i} + \frac{V_{\text{hom}}^l}{V_{\text{hom}}^g} \sum_i e_{\text{pure}}^{l,i} N_{\text{hom}}^{g,i}. \end{aligned} \quad (55)$$

In the previous versions<sup>13,17,18</sup> of the second homogeneous nucleation theory, the terms proportional to  $V_{\text{hom}}^l/V_{\text{hom}}^g$  have

been omitted as negligible, or because the reference state used has been an empty system rather than the cluster volume filled with gas. These terms represent the energy of the molecules that the cluster space would have if filled with gas, and the energy those molecules in pure bulk liquids, and are indeed small, since the cluster occupies a tiny portion of the total volume of the nucleating gas, but we have included these terms here to be consistent with our general formalism.

Using result (48) and relations  $A_{g,l}^{\text{het}}/A_{g,l}^{\text{hom}} N_{g,l,\text{hom}}^{\text{surf},i} = N_{g,l,\text{het}}^{\text{surf},i}$ ,  $A_{g,l}^{\text{het}}/A_{g,l}^{\text{hom}} U_{g,l,\text{hom}}^{\text{surf}} = U_{g,l,\text{het}}^{\text{surf}}$ ,  $f_N N_{\text{hom}}^{l,i} = N_{\text{het}}^{l,i}$ ,  $f_N V_{\text{hom}}^l = V_{\text{het}}^l$ , and

$f_N U_{\text{hom}}^l = U_{\text{het}}^l$  we get the result

$$\begin{aligned} \left( \frac{\partial(-\Delta G_{\text{het}}^*)}{\partial T} \right)_{A_{g,i}} &= f_N \left( \frac{U_{\text{hom}}^l - \sum_i e_{\text{pure}}^{l,i} N_{\text{hom}}^{l,i}}{kT^2} + \frac{-\frac{V_{\text{hom}}^l}{V_{\text{hom}}^g} U^g + \frac{V_{\text{hom}}^l}{V_{\text{hom}}^g} \sum_i e_{\text{pure}}^{l,i} N_{\text{hom}}^{g,i}}{kT^2} \right) + \left[ f_N - \frac{1}{3} \left( m \frac{\partial f_G}{\partial m} - \frac{X}{2} \frac{\partial f_G}{\partial X} \right) \right] \\ &\quad \times \frac{U_{g,l,\text{hom}}^{\text{surf}} - \sum_i e_{\text{pure}}^{l,i} N_{g,l,\text{hom}}^{\text{surf},i}}{kT^2} - \left( \frac{U_{g,\text{sol},A_{l,\text{sol}}}^{\text{surf}} - \sum_i e_{\text{pure}}^{l,i} N_{g,\text{sol},A_{l,\text{sol}}}^{\text{surf},i}}{kT^2} \right) + \frac{U_{l,\text{sol}}^{\text{surf}} - \sum_i e_{\text{pure}}^{l,i} N_{l,\text{sol}}^{\text{surf},i}}{kT^2} \\ &= f_N \left( \frac{U_{\text{hom}}^l - \sum_i e_{\text{pure}}^{l,i} N_{\text{hom}}^{l,i}}{kT^2} + \frac{-\frac{V_{\text{hom}}^l}{V_{\text{hom}}^g} U^g + \frac{V_{\text{hom}}^l}{V_{\text{hom}}^g} \sum_i e_{\text{pure}}^{l,i} N_{\text{hom}}^{g,i}}{kT^2} \right) + \frac{A_{g,l}^{\text{het}}}{A_{g,l}^{\text{hom}}} \left( \frac{U_{g,l,\text{hom}}^{\text{surf}} - \sum_i e_{\text{pure}}^{l,i} N_{g,l,\text{hom}}^{\text{surf},i}}{kT^2} \right) \\ &\quad - \left( \frac{U_{g,\text{sol},A_{l,\text{sol}}}^{\text{surf}} - \sum_i e_{\text{pure}}^{l,i} N_{g,\text{sol},A_{l,\text{sol}}}^{\text{surf},i}}{kT^2} \right) + \frac{U_{l,\text{sol}}^{\text{surf}} - \sum_i e_{\text{pure}}^{l,i} N_{l,\text{sol}}^{\text{surf},i}}{kT^2} \\ &= \frac{1}{kT^2} \left( U_{\text{het}}^l + U_{g,l,\text{het}}^{\text{surf}} + U_{l,\text{sol}}^{\text{surf}} - \frac{V_{\text{het}}^l}{V_{\text{hom}}^g} U^g - U_{g,\text{sol},A_{l,\text{sol}}}^{\text{surf}} - \sum_i e_{\text{pure}}^{l,i} N_{\text{het}}^{l,i} - \sum_i e_{\text{pure}}^{l,i} N_{g,l,\text{het}}^{\text{surf},i} - \sum_i e_{\text{pure}}^{l,i} N_{l,\text{sol}}^{\text{surf},i} \right. \\ &\quad \left. + \frac{V_{\text{het}}^l}{V_{\text{hom}}^g} \sum_i e_{\text{pure}}^{l,i} N_{\text{hom}}^{g,i} + \sum_i e_{\text{pure}}^{l,i} N_{g,\text{sol},A_{l,\text{sol}}}^{\text{surf},i} \right), \end{aligned} \quad (56)$$

which is equal to formula (23) since we study the homogeneous and heterogeneous nucleation in the same vapor, and thus  $N_{\text{hom}}^{g,i}/V_{\text{hom}}^g = N_{\text{het}}^{g,i}/V_{\text{het}}^g = \rho_{g,i}$ . Thus, we have explicitly shown that the Fletcher<sup>14</sup> theory is also consistent with the second nucleation theorem.

## VI. THEOREMS IN TERMS OF THE NUCLEATION PROBABILITY

So far, the forms of nucleation theorems presented in the literature have only linked the behavior of the nucleation rate to the critical cluster properties. In heterogeneous nucleation experiments the quantity of prime interest is, however, the nucleation probability, which tells the fraction of pre-existing particles that have a nucleated cluster growing on the surface. We want to link this directly observable quantity to the properties of the clusters. From the definition of the nucleation probability  $P$  in a time period  $t$  (see, for example, Ref. 19)

$$P = 1 - \exp(-J_{\text{het}} \cdot t), \quad (57)$$

we get

$$\ln J_{\text{het}} = \ln \left( \ln \left( \frac{1}{1-P} \right) \right) - \ln t, \quad (58)$$

where  $J_{\text{het}}$  is the nucleation rate per pre-existing particle per unit time (units 1/s). To obtain the nucleation probability as functions of the gas phase activities as in Fig. 2 the experimentalist count the number of pre-existing particles which have activated as nucleation centers and started to grow after a certain fixed time. To get the probability curve as a function of the vapor activity, the latter is changed, but the time period after which the probability measured is kept constant. Thus, we can keep  $t$  constant when analyzing this kind of experimental data. We take the differential of Eq. (58) with respect to  $\ln A_{i,g}$  and  $T$  using the fact that the nucleation rate is connected to the formation energy by  $J_{\text{het}} = K \exp(-\Delta G_{\text{het}}/kT)$ , where  $K$  is a kinetic pre-factor. We can express the heterogeneous nucleation theorems as

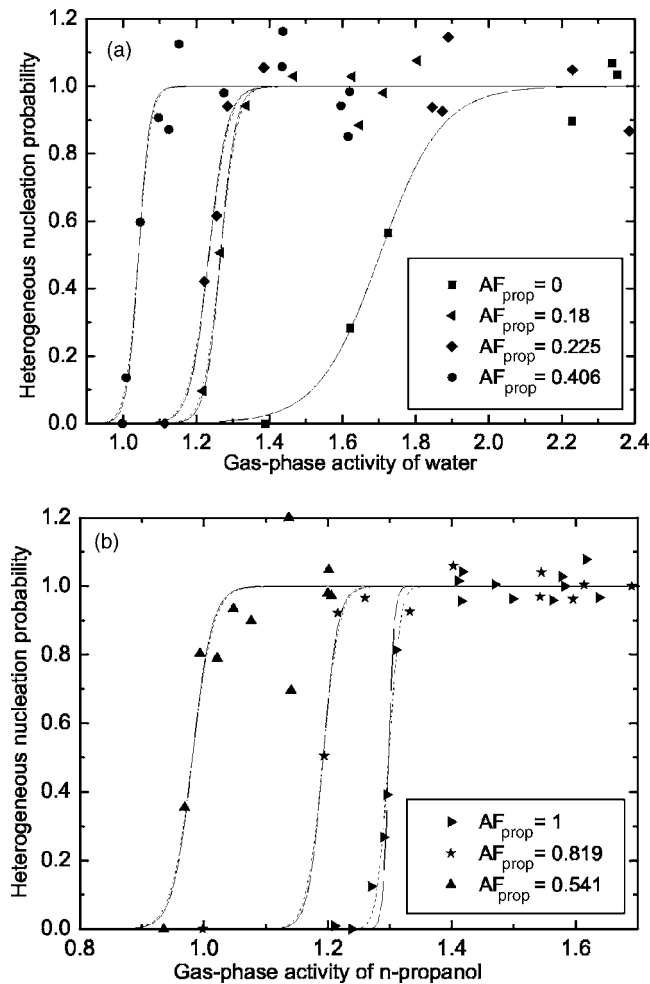


FIG. 2. The experimental nucleation probabilities (markers), fit functions for monodisperse 8 nm seed particles (solid lines) and integrated probabilities for the actual experimental particle size distribution (dash-dotted lines). The top figure shows the water-rich cases, and the bottom figure the *n*-propanol rich cases. Different markers are used for different gas-phase fractions of *n*-propanol given in the legends. The *x*-axis shows the gas-phase activity of water (top figure) or *n*-propanol (bottom figure).

$$\begin{aligned} \left( \frac{\partial \ln(\ln \frac{1}{1-P})}{\partial \ln \mathcal{A}_{g,i}} \right)_{T, \mathcal{A}_{g,j \neq i}} &\equiv \left( \frac{\partial F}{\partial \ln \mathcal{A}_{g,i}} \right)_{T, \mathcal{A}_{g,j \neq i}} \\ &= \left( \frac{\partial \ln J_{\text{het}}}{\partial \ln \mathcal{A}_{g,i}} \right)_{T, \mathcal{A}_{g,j \neq i}} = \Delta N_{\text{het},i}^* \\ &\quad + \left( \frac{\partial \ln K}{\partial \ln \mathcal{A}_{g,i}} \right)_{T, \mathcal{A}_{g,j \neq i}}, \end{aligned} \quad (59)$$

$$\begin{aligned} \left( \frac{\partial \ln(\ln \frac{1}{1-P})}{\partial T} \right)_{\mathcal{A}_{g,i}} &\equiv \left( \frac{\partial F}{\partial T} \right)_{\mathcal{A}_{g,i}} = \left( \frac{\partial \ln J_{\text{het}}}{\partial T} \right)_{\mathcal{A}_{g,i}} \\ &= \Delta(\Delta_{\text{pure},l} U^*) + \left( \frac{\partial \ln K}{\partial T} \right)_{\mathcal{A}_{g,i}}, \end{aligned} \quad (60)$$

which link experimentally accessible nucleation probability  $P$  to quantitative properties of critical clusters growing on particle surfaces. We have defined  $F \equiv \ln[\ln 1/(1-P)]$  to shorten the notation later in this paper. Note that  $F$  only has meaningful values when the nucleation probability is greater

than zero but less than one, and this is the range of experimental results we can use to obtain critical cluster properties.

## VII. KINETIC PRE-FACTOR

In the multicomponent nucleation the contribution of the pre-factor  $K$  cannot be exactly calculated,<sup>18</sup> but the classical form of the kinetic pre-factor  $K$  can be used to estimate the effect of the kinetics on the nucleation theorems. According to the classical theory the pre-factor (for nucleation rate per pre-existing particle, units 1/s) reads

$$K = 4 \pi R_p^2 R_{\text{av}} c_{s,\text{tot}}^{\text{ads}} Z. \quad (61)$$

The total number of molecules adsorbed on the pre-existing particle surface is  $c_{s,\text{tot}}^{\text{ads}} = c_{s,1}^{\text{ads}} + c_{s,2}^{\text{ads}}$ , and the expressions for  $c_{s,i}^{\text{ads}}$  (1/m<sup>2</sup>) are calculated using a steady state between incoming and outgoing molecule fluxes<sup>20</sup>

$$c_{s,i}^{\text{ads}} = \frac{p_{g,i}}{v_i \sqrt{2 \pi k T m_i}} \exp\left( \frac{-\Delta F_{\text{des},i}}{kT} \right), \quad (62)$$

where  $m_i$  is the mass of a molecule,  $p_{g,i}$  is the pressure in the nucleating vapor,  $v_i$  is the vibration frequency of a molecule on the surface, and  $\Delta F_{\text{des},i}$  is the desorption energy for component  $i$ .

The average growth rate  $R_{\text{av}}$  is defined as

$$R_{\text{av}} = \frac{\beta_1^{\text{het}} \beta_2^{\text{het}}}{\beta_1^{\text{het}} \sin^2 \Upsilon + \beta_2^{\text{het}} \cos^2 \Upsilon}. \quad (63)$$

$\Upsilon$  is the direction angle of the critical cluster growth vector obtained as the eigenvector associated with the negative eigenvalue of the matrix product  $R^* \cdot W^*$ , where the growth matrix containing the collision rates  $\beta_i^{\text{het}}$  is

$$R^* = \begin{pmatrix} \beta_1^{\text{het}} & 0 \\ 0 & \beta_2^{\text{het}} \end{pmatrix}. \quad (64)$$

Matrix  $W^*$  is formed from the second derivatives of the formation free energy

$$W^* = \begin{pmatrix} \left( \frac{\partial^2 \Delta G_{\text{het}}}{\partial n_1^2} \right)^* & \left( \frac{\partial^2 \Delta G_{\text{het}}}{\partial n_1 \partial n_2} \right)^* \\ \left( \frac{\partial^2 \Delta G_{\text{het}}}{\partial n_1 \partial n_2} \right)^* & \left( \frac{\partial^2 \Delta G_{\text{het}}}{\partial n_2^2} \right)^* \end{pmatrix} \equiv \begin{pmatrix} W_{11}^* & W_{12}^* \\ W_{12}^* & W_{22}^* \end{pmatrix}, \quad (65)$$

with the derivatives performed with respect to the total numbers in the heterogeneous cluster.<sup>21</sup> The total numbers of molecules consist of bulk liquid contributions plus surface excess corrections for both gas-liquid and liquid-solid interfaces.

The direct vapor deposition approach<sup>22</sup> takes into account only the vapor monomers colliding directly with the critical cluster, whereas the surface diffusion approach<sup>20</sup> considers only the monomers that have collided and adhered to the surface of the pre-existing particle, after which they diffuse to the cluster. The surface diffusion approach is used in this model, and it gives 7–8 orders of magnitude higher collision rates than the direct vapor deposition model. The collision rates  $\beta_i^{\text{het}}$  (1/s) are given as the product of the number



of adsorbed molecules in position to join the germ, and the frequency  $\nu_i \exp(-\Delta F_{sd,i}/kT)$  with which they jump to join it

$$\beta_i^{\text{het}} = 2\pi R_p \sin \varphi D c_{s,i}^{\text{ads}} \nu_i \exp\left(\frac{-\Delta F_{sd,i}}{kT}\right), \quad (66)$$

where  $D$  is the mean jump distance of a molecule, and  $\Delta F_{sd,i}$  is the surface diffusion energy. The length of the circular contact line between the gas, liquid and solid is calculated as  $R_p \sin \varphi$ ,<sup>14</sup> with the angle  $\varphi$  given by  $\cos \varphi = (X-m)/g$ .

The Zeldovich factor  $Z$  appearing in the formula (61) is given by

$$Z = \frac{-(W_{11}^* + 2W_{12}^* \tan Y + W_{22}^* \tan^2 Y)}{1 + \tan Y} \frac{1}{\sqrt{|\det W^*|}}. \quad (67)$$

Detailed description of the kinetics of multicomponent heterogeneous nucleation is presented by Määttänen *et al.*,<sup>21</sup> and the parameters used for water-*n*-propanol mixture are the same as used by Kulmala *et al.*<sup>23</sup> In all classical calculations, unless otherwise stated, we have used the microscopic contact angle<sup>24</sup>

$$\theta = \frac{35.82^\circ (1-x)}{(1+61.62x)}, \quad (68)$$

where  $x$  is the mole fraction of *n*-propanol in the liquid.

### VIII. EXPERIMENTAL DATA

No experimental data so far is available for the application of the second heterogeneous nucleation theorem; here we demonstrate the power of the first theorem in a practical application. In recent experiments Wagner *et al.*<sup>24</sup> have obtained nucleation probabilities for unary and binary heterogeneous nucleation of water and *n*-propanol vapors on silver nanoparticles. Nearly monodispersed populations of Ag particles with a geometric mean particle diameter of 8 nm and geometric standard deviation 1.035 were used as seed particles. This geometric standard deviation is somewhat smaller as compared to the value reported previously.<sup>24</sup> The smaller geometric standard deviation of the seed particles has actually been determined in the present study by more accurate accounting for the transfer function of the electrostatic aerosol classifier<sup>25</sup> used in the experiments. The experiments were conducted with several gas-phase activity fractions of *n*-propanol

$$X_g = A_{g,2}/(A_{g,1} + A_{g,2}), \quad (69)$$

$X_g=0$  (pure water), 0.18, 0.225, 0.406, 0.541, 0.725, 0.819, and 1 (pure *n*-propanol). Although the Ag particles are quite narrowly distributed, the influence of the finite width of the particle size distribution on the measured nucleation probabilities must be taken into account. For extracting the influence of polydispersity, we consider nucleation probability functions  $P$  for strictly monodispersed particles, which, for a constant activity fraction  $X_g$  can be approximately expressed by the formula

TABLE I. Lambda values that fit Eq. (70) to the experimental data for different gas-phase activity fractions  $X_g$ . The table also shows the mass fractions of *n*-propanol  $X_{M,l}$  in the liquid used to generate the nucleating vapor.

$X_g$	$X_{M,l}$	$\lambda_1$	$\lambda_2$
0.0	0	5.93	-10.09
0.18	0.376	23.86	-30.95
0.225	0.446	19.19	-24.69
0.406	0.653	27.11	-34.22
0.541	0.763	24.20	-31.16
0.819	0.926	42.05	-51.34
1.0	1.0	115.85	-150.37

$$P = \frac{1}{2} \tanh(\lambda_1 A_g + \lambda_2) + \frac{1}{2}, \quad (70)$$

where  $A_g = \sqrt{A_{g,2}^2 + A_{g,1}^2}$  is used as a representative value corresponding to the gas phase activities in the binary vapor mixture. The parameter  $\lambda_1$  is related to the slope of the nucleation probability  $P$  when plotted as a function of mean gas-phase activity  $A_g$ . This slope is assumed to be independent of the particle size over the narrow range of particle sizes considered in the experiments. The ratio  $-\lambda_2/\lambda_1$  is the onset saturation ratio corresponding to nucleation probability  $P=0.5$ . This onset saturation ratio has been obtained as a function of the particle diameter from additional nucleation measurements performed for Ag particles with diameters slightly above and below 8 nm. Integration of the nucleation probability functions  $P$  for strictly monodispersed particles over the actual experimental particle size distribution yields an integrated nucleation probability function, which can be directly compared to the experimental results. The experimental data points can be fitted by appropriate choice of  $\lambda_1$ . Each experimental gas-phase activity fraction  $X_g$  is thus associated with a  $(\lambda_1, \lambda_2)$  pair listed in Table I as a result of the fitting. It should be noted that this procedure is not dependent on any specific theoretical model.

Figure 2 shows the experimental data and the fitted nucleation probability functions  $P$  for monodisperse 8 nm seed particles (solid lines). Integration of the nucleation probability functions  $P$  over the actual experimental particle size distribution results in integrated nucleation probability functions (dashed lines) in good agreement with experiments.

The numbers of molecules in the critical cluster  $\Delta N_{\text{het},i}^*$  are calculated from the experimentally determined nucleation probability function  $P$  for strictly monodispersed particles, Eq. (70). From the fit functions to the experimental data, we can determine the derivative  $(\partial F/\partial A_g)_{X_g}$  which according to Strey, Viisanen, and Wagner<sup>26,27</sup> can be used to calculate the derivatives needed in the first nucleation theorem (59) as

$$\left(\frac{\partial F}{\partial \ln \mathcal{A}_{g,1}}\right)_{T, \mathcal{A}_{g,2}} = \mathcal{A}_{g,1} \left(\frac{\partial F}{\partial \mathcal{A}_g}\right)_{X_g} \cdot \left(\frac{\partial \mathcal{A}_{g,2}}{\partial \mathcal{A}_{g,1}}\right)_F \cdot \frac{\sqrt{1 + \left(\frac{\partial \mathcal{A}_{g,2}}{\partial \mathcal{A}_{g,1}}\right)_F^2 - (A_{g,2}/A_{g,1})^2}}{\left(\frac{\partial \mathcal{A}_{g,2}}{\partial \mathcal{A}_{g,1}}\right)_F - (A_{g,2}/A_{g,1})}, \quad (71)$$

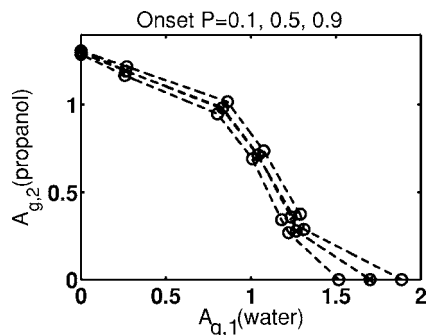


FIG. 3. Gas-phase activities that give a constant nucleation probability  $P$ . The lowest curve is related to the lowest probability. The circles mark the values obtained for experimental gas-phase activity ratio from Eq. (70), the dashed lines the results of the interpolation, and the crosses, which accurately overlap the  $P=0.5$  circles, are the measured experimental onset activities for  $P=0.5$ .

$$\left(\frac{\partial F}{\partial \ln \mathcal{A}_{g,2}}\right)_{T, \mathcal{A}_{g,1}} = \mathcal{A}_{g,2} \cdot \left(\frac{\partial F}{\partial \mathcal{A}_g}\right)_{X_g} \cdot \frac{\sqrt{1 + (\mathcal{A}_{g,2}/\mathcal{A}_{g,1})^2}}{(\mathcal{A}_{g,2}/\mathcal{A}_{g,1}) - \left(\frac{\partial \mathcal{A}_{g,2}}{\partial \mathcal{A}_{g,1}}\right)_F}, \quad (72)$$

with  $F$  defined as

$$F \equiv \ln[\ln 1/(1-P)]. \quad (73)$$

We thus need the derivative  $(\partial \mathcal{A}_{g,2}/\partial \mathcal{A}_{g,1})_F$  for the onset curve with constant  $F$  (in other words constant nucleation probability  $P$ ). Gas-phase activity  $\mathcal{A}_{g,2}$  as a function of  $\mathcal{A}_{g,1}$  for any constant  $P$  can be solved from Eq. (70) analytically for the experimental gas-phase activity fractions. To obtain the derivatives we need  $\mathcal{A}_{g,2}(\mathcal{A}_{g,1})$  also for activity fractions slightly off the experimental values, and we have used table look-up linear interpolation scheme<sup>28</sup> to obtain these intermediate values. Figure 3 shows the onset curves for nucleation probabilities 0.1, 0.5, and 0.9.

## IX. RESULTS

The sub-plots of Fig. 4, each representing a constant gas-phase activity fraction, show the numbers of molecules in the critical cluster extracted from the experimental data using the first nucleation theorem (59). The molecular numbers are (with a couple of exceptions at the left end of the  $x$  axis where  $P$  approaches zero) smooth monotonous functions of gas-phase activities, as is physically reasonable. We also show the classical theory predictions for comparison. The classical theory gives orders of magnitude larger critical cluster than the analysis of the experimental data. If the macroscopic contact angles are used instead of the microscopic ones, the classical clusters contain in some cases even more molecules. We have limited the  $y$ -axes and thus left out some classical values to better show the experimental results. It has been shown earlier,<sup>24</sup> that the classical theory predicts well the onset conditions for heterogeneous nucleation but the present analysis shows that the transition from nucleation probability value 0 to value 1 is in reality not as steep as the classical model prediction. We checked the correctness and consistency of our data analysis by checking that at the one-component limit, the two-component theorems also in practice give the results obtained by one-component analysis;

this check also assured us that the fit based on Eq. (70) behaves well at the one-component limits.

Using classical formulas the derivative of the kinetic pre-factor  $\ln K$  with respect to  $\ln \mathcal{A}_{g,i}$  can be estimated numerically. For the range of experimental conditions it yields 3–8 for pure water, 8–16 for pure  $n$ -propanol (this estimate is obtained using the macroscopic contact angle  $19.1^\circ$ , microscopic zero contact angle leads to infinite values and, for example,  $\theta=1^\circ$  leads to values 2–120), and 2–11 for the binary cases with the derivatives taken with respect to both gas-phase activities. As a further check of our theorem, and also the correctness of derivatives of the kinetic pre-factor, we also have generated nucleation probability data with the classical heterogeneous nucleation theory, applied the heterogeneous nucleation theorem to this data, and checked that the resulting numbers of molecules in the critical cluster are equal to the numbers of molecules given by the classical theory.

Somewhat surprisingly, the kinetic contribution to the first nucleation theorem is not in the range of 1–2 as in the homogeneous one and two-component cases.<sup>13,17,18</sup> This can be understood, for simplicity in a one-component system, by comparing Eq. (61) to the homogeneous counterpart

$$K_{\text{hom}} = c_1 \beta^{\text{hom}} Z_{\text{hom}}, \quad (74)$$

where  $c_1$  is the number of monomers in the nucleating vapor. The monomer concentration is proportional to the gas-phase activity,  $c_1 \propto p_g \propto \mathcal{A}_g$ , the collision rate between critical clusters and monomers is proportional to the monomer concentration and the surface area of the cluster,  $\beta^{\text{hom}} \propto p_g^2 4\pi r^{*2} \propto \mathcal{A}_g r^{*2}$ , and the Zeldovich factor is inversely proportional to the area of the cluster<sup>29</sup>  $Z_{\text{hom}} \propto 1/r^{*2}$ . In all these cases the proportionality constants do not depend on the gas-phase activity  $\mathcal{A}_g$ . Thus the dependence of the kinetic factor on the radius of the critical cluster cancels out,  $K_{\text{hom}} \propto \mathcal{A}_g^2$ , and the contribution of the pre-factor equals 2 ( $K_{\text{hom}} = c_1 \beta^{\text{hom}} Z_{\text{hom}} / \mathcal{A}_g$  in the “1/S-version” of the classical theory,<sup>30</sup> in which case the contribution is 1). In the heterogeneous (again for simplicity one-component) case Eq. (62) gives,  $c_s^{\text{ads}} \propto \mathcal{A}_g$ , Eqs. (63) and (66) yield  $R_{\text{av}} = \beta^{\text{het}} \propto \sin \varphi c_s^{\text{ads}} \propto \sin \varphi \mathcal{A}_{g,i}$ , where  $\cos \varphi = (X-m)/\sqrt{1-2mX+X^2}$  and  $X = R_p/r^*$ , and the Zeldovich factor also depends on the critical cluster radius as<sup>31</sup>

$$Z \propto 1/r^{*2} \sqrt{\frac{4}{\left(2 + \frac{(1-mX)[2-4mX-(m^2-3)X^2]}{(1-2mX+X^2)^{3/2}}\right)}}. \quad (75)$$

Thus the kinetic pre-factor depends on the gas-phase activity  $\mathcal{A}_g$  in a complicated way

$$K \propto \mathcal{A}_g^2 / r^{*2} \sin \varphi \sqrt{\frac{4}{\left(2 + \frac{(1-mX)[2-4mX-(m^2-3)X^2]}{(1-2mX+X^2)^{3/2}}\right)}}, \quad (76)$$

with  $X = R_p/r^*$ , and  $r^*$  depending on the gas phase activity according to the Kelvin Eq. (25). The nonspherical geometry of the cluster, and the fact that the contact line between the substrate and the cluster plays the same role in the collision rate as the surface area of the cluster in the homogeneous case, result in the dependency of  $K$  on  $r^*$  not canceling out,

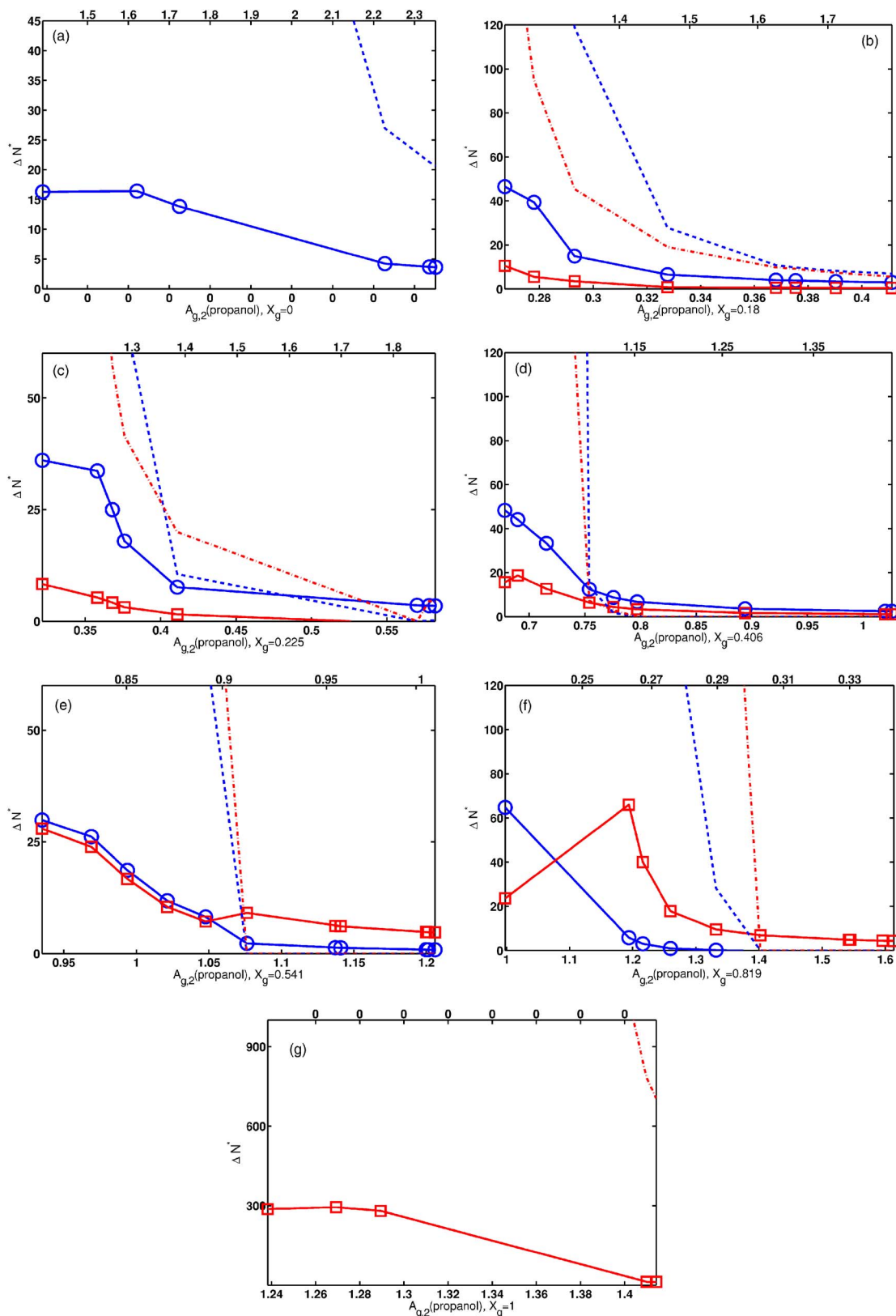


FIG. 4. (Color online) Numbers of molecules in the critical cluster obtained from the experimental data using the first nucleation theorem. Solid lines with circles refer to water molecules, solid lines with squares to *n*-propanol. Classical theory predictions for water are indicated by dashed lines, and for *n*-propanol by dot-dashed lines. The seven sub-plots show data for different gas-phase activity fractions ( $X_g$ ) marked below each plot. The bottom *x*-axes show the gas-phase activity of *n*-propanol, while the top *x*-axes give the gas-phase activity of water.

and thus the contribution of the pre-factor differs from the homogeneous case. Test calculations show that the contribution of the pre-factor is sensitive to the critical cluster size, as well as to the contact angle: the values obtained using the

classical theory for very large clusters are not applicable to the experimental results with much smaller cluster sizes. Subtraction of the classical values for the kinetic contribution from the results given by the data analysis would lead to

negative numbers when the experiments indicate the clusters to be small. Thus, in Fig. 4 the effect of the kinetic pre-factor has not been taken into account. A more sophisticated model for the kinetics is needed to estimate the role of the kinetic pre-factor in the heterogeneous nucleation theorem.

For pure water the critical clusters contain less than 17 molecules, for pure *n*-propanol the largest clusters have around 300 molecules. This difference in the critical cluster sizes of pure components follows directly from the clearly steeper slope of nucleation probability for pure *n*-propanol compared to that of pure water in Fig. 2. For gas-phase activity ratios  $X_g=0.18$ , 0.225, and 0.406 clusters contain more water than *n*-propanol, for  $X_g=0.541$  half of the cluster molecules are water, half *n*-propanol, and for  $X_g=0.819$  *n*-propanol clearly dominates. The largest binary clusters contain less than 90 molecules. Our analysis demonstrates that the experimentally obtained heterogeneous nucleation probability does not change too steeply as a function of the gas-phase activity, thus allowing a meaningful data analysis.

## X. CONCLUSIONS

The formation of new small clusters on seed particles has earlier been studied in well-defined experiments.<sup>24</sup> This paper shows how these experiments can be utilized to identify the size of newly formed molecular clusters using the first heterogeneous nucleation theorem. The clusters studied typically contain only 10–100 molecules. The critical cluster sizes obtained from the experiments using the heterogeneous nucleation theorem are dramatically smaller than the predictions by the classical nucleation theory. This result is related to the fact that the slopes of the nucleation probability curves given by the classical nucleation theory<sup>14</sup> are generally found to be considerably steeper compared to the experimental data.<sup>24</sup> The discrepancy between the classical theory and experiments clearly indicates that the nucleating clusters are too small to be quantitatively described using the macroscopic Fletcher theory.<sup>14</sup> The clusters are on the verge of a full quantum mechanical description to be computationally feasible. The heterogeneous nucleation theorems provide direct experimental access to nanocluster properties. In the future, when heterogeneous nucleation experiments will be conducted at various temperatures, the second nucleation theorem provides the means to analyze the energetics of the clusters, and aid the development of accurate models for molecular interactions between the nucleating molecules, and between the cluster and the underlying surfaces. The application of heterogeneous nucleation theorems leads to an improved understanding of nanocluster formation.

## ACKNOWLEDGMENTS

The assistance of Kai Ruusuvoori is gratefully acknowledged. This work was supported by the Academy of Finland and the Austrian Science Foundation, Project No. P16958-N02. We thank Professor G. P. Reischl for his valuable help with the determination of the experimental seed particle size distribution.

- <sup>1</sup>P. Hamill, R. P. Turco, C. S. Kiang, O. B. Toon, and R. C. Whitten, *J. Aerosol Sci.* **13**, 561 (1982).
- <sup>2</sup>H. Korhonen, K. Lehtinen, and M. Kulmala, *Atmos. Chem. Phys.* **4**, 757 (2004).
- <sup>3</sup>R. J. Charlson, S. E. Schwartz, J. M. Hales, R. D. Cess, J. A. Coakley, J. E. Hansen, and D. J. Hofmann, *Science* **255**, 423 (1992).
- <sup>4</sup>P. A. Stott, S. F. B. Tett, G. S. Jones, M. R. Allen, J. F. B. Mitchell, and G. J. Jenkins, *Science* **290**, 2133 (2000).
- <sup>5</sup>V. Ramanathan, P. J. Crutzen, J. T. Kiehl, and D. Rosenfeld, *Science* **294**, 2119 (2001).
- <sup>6</sup>S. Menon, A. D. Del Genio, D. Koch, and G. Tselioudis, *J. Atmos. Sci.* **59**, 692 (2002).
- <sup>7</sup>M. Kulmala, K. E. J. Lehtinen, and A. Laaksonen, *Atmos. Chem. Phys.* **6**, 787 (2006).
- <sup>8</sup>D. Kashchiev, *Nucleation: Basic Theory with Applications* (Butterworth-Heinemann, Oxford, 2000).
- <sup>9</sup>S. Toschev, *Crystal Growth: An Introduction* (North-Holland, Amsterdam, 1973).
- <sup>10</sup>D. W. Oxtoby and D. Kashchiev, *J. Chem. Phys.* **100**, 7665 (1994).
- <sup>11</sup>H. Reiss, *Methods of Thermodynamics* (Dover, New York, 1996).
- <sup>12</sup>F. F. Abraham, *Advances in Theoretical Chemistry* (Academic, New York, 1974).
- <sup>13</sup>I. J. Ford, *J. Chem. Phys.* **105**, 8324 (1996).
- <sup>14</sup>N. Fletcher, *J. Chem. Phys.* **29**, 572 (1958).
- <sup>15</sup>T. Young, *Philos. Trans. R. Soc. London* **95**, 65 (1805).
- <sup>16</sup>A. Määttänen, H. Vehkamäki, A. Lauri, S. Merikallio, J. Kauhanen, H. Savijärvi, and M. Kulmala, *J. Geophys. Res.* **110**, E02002 (2005).
- <sup>17</sup>I. J. Ford, *Phys. Rev. E* **56**, 5615 (1997).
- <sup>18</sup>H. Vehkamäki and I. J. Ford, *J. Chem. Phys.* **113**, 3261 (2000).
- <sup>19</sup>M. Lazaridis, M. Kulmala, and B. Z. Gorbunov, *J. Aerosol Sci.* **23**, 457 (1992).
- <sup>20</sup>H. R. Pruppacher and J. D. Klett, *Microphysics of Clouds and Precipitation* (Kluwer, Norwell, Massachusetts, 1997).
- <sup>21</sup>A. Määttänen, H. Vehkamäki, A. Lauri, I. Napari, and M. Kulmala, *J. Chem. Phys.* (to be published).
- <sup>22</sup>A. Inada, Ph.D. thesis, Kobe University, Japan (2002).
- <sup>23</sup>M. Kulmala, A. Lauri, H. Vehkamäki, A. Laaksonen, D. Petersen, and P. E. Wagner, *J. Phys. Chem. B* **105**, 11800 (2001).
- <sup>24</sup>P. Wagner, D. Kaller, A. Vrtala, A. Lauri, M. Kulmala, and A. Laaksonen, *Phys. Rev. E* **67**, 021605 (2003).
- <sup>25</sup>G. P. Reischl, J. M. Mäkelä, and J. Nécid, *Aerosol Sci. Technol.* **27**, 651 (1997).
- <sup>26</sup>R. Strey and Y. Viisanen, *J. Chem. Phys.* **99**, 4693 (1993).
- <sup>27</sup>R. Strey, Y. Viisanen, and P. E. Wagner, *J. Chem. Phys.* **103**, 4333 (1995).
- <sup>28</sup>Matlab Reference Guide, Version 7.1.0.183 (R14) Service Pack 3 (The MathWorks, Inc., MA, 2005).
- <sup>29</sup>H. Vehkamäki, *Classical Nucleation Theory in Multicomponent Systems* (Springer, Berlin, Heidelberg, 2006).
- <sup>30</sup>H. Reiss, W. K. Kegel, and J. I. Katz, *Phys. Rev. Lett.* **78**, 4506 (1997).
- <sup>31</sup>H. Vehkamäki, A. Määttänen, A. Lauri, I. Napari, and M. Kulmala, *Atmos. Chem. Phys.* **7**, 309 (2007).